WILEY | Hindawi

Research Article

Simulation and Analysis of a Split Drill Bit for Pneumatic DTH Hammer Percussive Rotary Drilling

Yuanling Shi [1,2] **and Conghui Li** [2]

[1]*Academician Workstation in Anhui Province, Anhui University of Science and Technology, Huainan 232001, China*
[2]*School of Earth and Environment, Anhui University of Science and Technology, Huainan 232001, China*

Correspondence should be addressed to Yuanling Shi; ylshi@aust.edu.cn

Reverse circulation impact drilling has the advantages of high drilling efficiency and less dust, which can effectively form holes in hard rock and gravel layer. As integral reverse circulation drill bits used in the conventional down-the-hole (DTH) hammers are only suitable for specific formations, the whole set of DTH hammer needs to be replaced when drilling different formations. In this paper, several types of split drill bits for different drilling technologies are designed. The flow field characteristics of one of the split drill bits is analyzed based on the computational fluid dynamics (CFD) method, with four technic parameters considered, which are input flow rate, number of inlet holes, angle of injection exhaust holes, and diameter of injection exhaust holes, respectively. Three parameters are selected as indicators to evaluate the rationality and performance of the split drill bit, which are injection exhaust hole outlet mass flow rate, ratio of the mass flow rate out of injection exhaust holes to the whole inlet mass flow rate, and maximum pressure at the upper end of the split drill bit. According to the CFD analysis results, the above four technic parameters influence the flow rate and pressure in different rules. Considering the injection capacity, pressure loss, and bit strength, inlet holes of 10, injection exhaust holes with an angle of 50°, and injection exhaust holes with a diameter of 12 mm are recommended to obtain ideal reverse circulation. Different types of split drill bits were manufactured, and drilling experiments were carried out in unconsolidated formations. The maximum drilling rate can reach 1.5 m/min in the drilling experiments. The split drill bit proposed in this paper exhibits excellent adaptability for reverse circulation drilling in loose formations.

1. Introduction

With the advantages of high drilling efficiency, minimal accidents, and good quality of borehole, percussive rotary drilling has found extensive applications in geological core drilling, solid mineral exploration, engineering geological exploration, geothermal drilling, and other fields and is gradually applied to oil and gas drilling [1–3]. During percussive rotary drilling process, a down-the-hole (DTH for short) hammer is used to generate impact energy, which is one of the most important components in percussive rotary drilling [4, 5]. The DTH air hammer utilizes compressed air as power to drive its piston moving up and down at high speed and impacting its drill bit, which cooperates with the rotary power from drilling rigs to realize percussive rotary

drilling [6, 7]. Due to several shortcomings, such as large gas consumption, more gas compression equipment required, serious borehole wall scouring, and grievous gas leakage in fractured formation, the application of normal circulation drilling with conventional DTH air hammer is somewhat constrained. Compared with the normal circulation DTH hammer, the distinctive feature of the reverse circulation DTH hammer is that it has a hollow structure. This hollow channel connects with the central passageways of dual-wall drill pipes, forming an upward reverse circulation pathway for rock cores, rock cuttings, and formation fluids. During reverse circulation drilling, compressed air is sent to the reverse circulation DTH hammer through the annulus clearance between the inner tubes and outer tubes of dual-wall drill pipes. Driven by compressed air, the piston inside

the DTH hammer impacts its drill bit repeatedly. Simultaneously, rock cuttings are discharged through the central hollow hole of the DTH hammer and the central passageways of the dual-wall drill pipes.

Different types of DTH air hammers and their drill bits have been designed and studied by numerous researchers [8, 9]. Zhukov et al. [10] designed a hammering piston of a DTH air hammer with curvilinear-free surfaces, and this structure ensures that there is no contact with the piston and the DTH body, so rock breaking impact is generated with the minimum energy input. Bo et al. [11] proposed a novel pneumatic DTH hammer, the biggest feature of which is that it has a self-propelled round bit. The purpose of designing this self-propelled round bit is to surmount the problems such as drilling tool wear in directional drilling, and working principles and performances of this new pneumatic DTH hammer are analyzed based on a nonlinear dynamic model. Zhang et al. [12] designed a reverse circulation drill bit with large diameter and numerically optimized the structure of the bit from the perspective of its suction capacity. To improve the rate of penetration (ROP) in downhole rescue drilling, Liu et al. [13] established a dynamic model for a pneumatic DTH hammer and acquired the velocity-displacement response of the drill bit's bottom in both time domain and frequency domain by integrating numerical simulation with engineering analysis. In literature [14], a large diameter reverse circulation DTH hammer was designed to improve the penetration rate for rescue well drilling, which was mainly used to deal with underground coal mine disasters. In literature [15], using multiphase fluid dynamic model, the transport and distribution of drilling cuttings were studied with different drilling parameters considered, and then, control performance of DTH drilling was evaluated. In literature [16], a reverse circulation drill bit was designed, which was used to deal with problems during drilling in complex formations; and then, drilling performance of the drill bit was studied during drilling fluid reverse circulation process based on numerical simulations and experiments. According to previous research, structural design and flow field analysis of DTH hammers are currently the main research topics. This is mainly because the structure of DTH hammers and fluid medium parameters determine the performance of the DTH hammers and the formation of reverse circulation. Computational fluid dynamics (CFD) is an approach for studying systems involving physical phenomena such as fluid flow through computer numerical calculation and visual representations [17, 18]. This method is particularly advantageous as it can be applied prior to the experiments, making it well suited for addressing flowing problems that may be challenging to implement experimentally. In contrast to experimental methods, full-field data can be obtained by CFD. Pressure, velocity, and other qualities of interest are available at every point in the simulated domain. What is more, CFD has unique advantages in solving flowing with characteristics of nonlinearity, multiple independent variables, and complex boundary conditions, which are difficult to obtain analytical expression by theoretical methods. It has been widely used in industries such as aerospace, nuclear industry, and oil and gas drilling [19–21]. When it comes to split drill bit design and analysis, because of the complex flow passageways in the bit, there will be a large computational workload with theoretical analysis. While conducting experimental research can impose high requirements for supporting conditions, such as drilling rigs, air compressors, and drilling experiment fields, this will extend the design and development cycle of drill bits, resulting in increased time and economic costs. With the advantages of convenient, economical, and efficient, CFD has emerged as one of the most promising methods for DTH hammer design and analysis.

Compared with rotary drilling, lower weight on bit (WOB) and slower speed of rotation are required for DTH drilling under the same stratum conditions [22, 23]. In air DTH hammer normal circulation drilling, compressed air is injected into the central passageways of drill pipes to drive DTH hammer working and carries rock cuttings out of the borehole along annulus clearance between drill pipes and borehole wall. In this process, a large amount of respirable dust is generated, resulting in environmental pollution and health risk to workers and potentially leading to pneumoconiosis. During DTH hammer reverse circulation drilling, compressed air flows inside dual-wall drill pipes to drive DTH hammer, which is profitable to maintain the stability of borehole wall. The outer tubes of the dual-wall drill pipes function as casing pipes, and the drill process is equivalent to drilling with casing. After powering the DTH hammer piston reciprocating, high-velocity air is ejected from the exhaust holes of drill bits at the bottom of the borehole and then flows upward into the central channel of the DTH hammer. Thus, the drilling cuttings can be discharged effectively using reverse circulation DTH hammer, and borehole bottom is clean, which is conducive to drill boreholes in extremely complex formation [24–26]. All cuttings discharged through reverse circulation can be transported to a specified location far from the drilling field through slag discharge pipes and collected by a cyclone separator. Therefore, there will be no dust flying, preventing environmental pollution and reducing the risk of prolonged worker exposure to dust [27, 28].

Currently, DTH hammer drill bits predominantly utilize integral structures, which exhibit certain drawbacks. Firstly, a singular integral bit is only suitable for specific drilling method and formations, limiting its versatility. If formations or drilling requirements change, necessitating a shift in drilling methods, the drill bit together with the DTH hammer must be replaced simultaneously. When drilling in complex formations, it needs to equip multiple DTH hammers to achieve different drilling processes, increasing equipment investment. Secondly, the traditional integral bits are machined from a steel piece, which is embedded with alloy teeth. The drill bit engages with the DTH hammer through splines to obtain rotary speed and torque from the drilling rig. Under the high-frequency impact of the DTH hammer piston, impact drilling is achieved through the interaction between alloy teeth and rock. During drilling process, due to factors such as improper operation and sudden changes in strata, accidents such as drill bit spline fracture, alloy tooth breakage, and alloy tooth detachment often occur, which will cause the entire drill bit to be scrapped, resulting
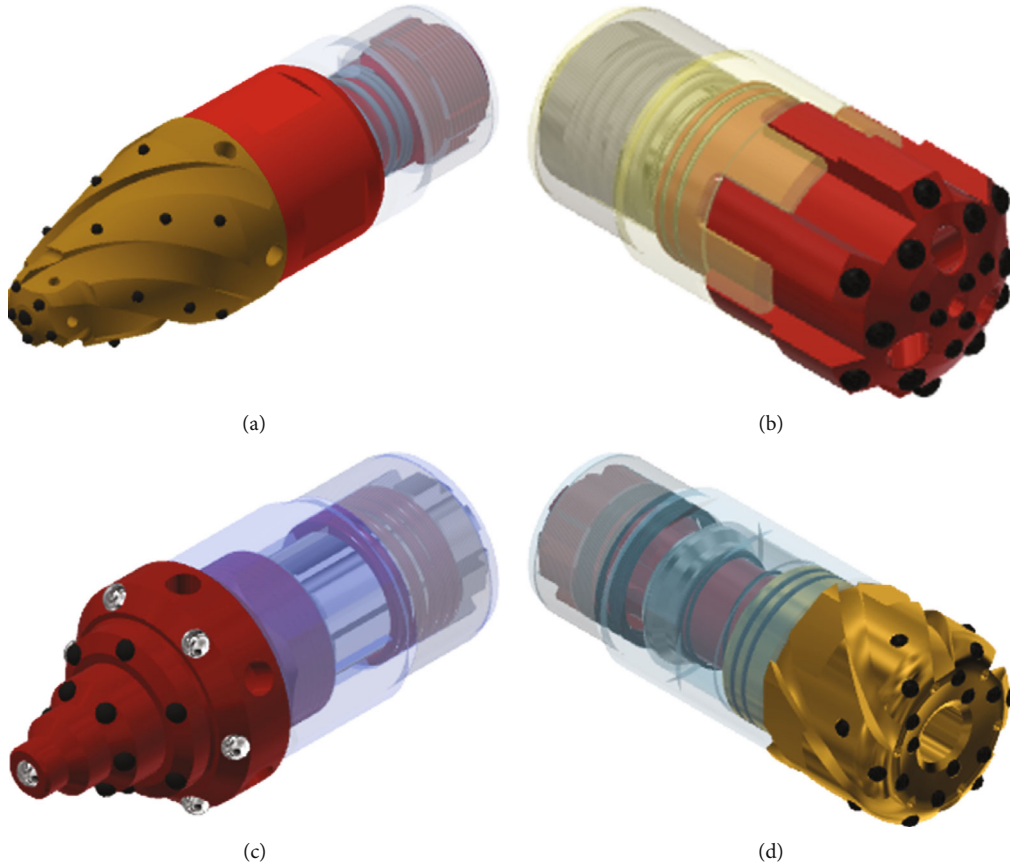
(a)

(b)

(c)

(d)

FIGURE 1: Drill bits of pneumatic DTH hammer for different drilling methods: (a) normal circulation bit; (b) reverse circulation bit; (c) percussion compact bit; (d) coring bit.

in high maintenance costs. What is more, machining the comprehensive gas distribution channels on the integral bit presents difficulties. Inadequate gas distribution channels result in subpar cooling for the alloy teeth and an unsatisfactory capacity to absorb drilling cuttings for reverse circulation drilling, which will accelerate the wear of the drill bit and reduce the drilling speed. Thus, several types of split drill bits for air DTH hammers are proposed in this paper to solve the above problems.

In this paper, several split drill bits for the DTH air hammer were designed and introduced firstly. In Section 3, a simulation model based on the CFD method was established in the ANSYS Workbench software. In Section 4, the working performance of the split reverse circulation bits is analyzed, with the mass flow rate, numbers of inlet holes, angle of injection exhaust holes, and diameter of injection exhaust holes considered. At the fifth section, field experiments were carried out in the gravel stratum in Sichuan Province to verify the performance of the split drill bits.

2. Structure Design of Split Drill Bits

To overcome the limitation of integral drill bits, several different split drill bits are designed. Constructions of normal circulation bit, reverse circulation bit, percussion compact bit, and coring bit are shown in Figure 1. When drilling with
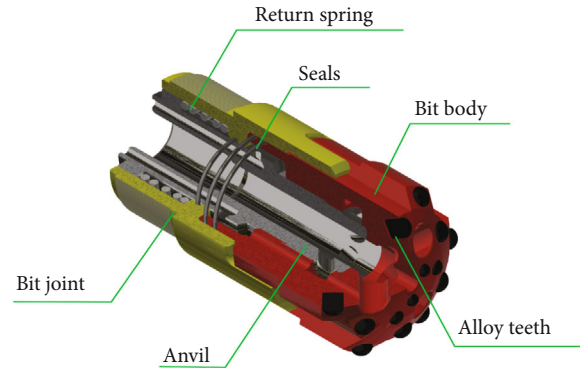

FIGURE 2: The split reverse circulation drill bit.

different targets, the specific drill bit can be connected to the same DTH hammer, so as to achieve different drilling methods by the same drilling tools and reducing equipment cost investment.

The above different types of drill bits have different structures. Taking the split drill bit for reverse circulation drilling, for example (in Figure 2), it is composed of an anvil with stepped cylindrical structure, a torque transmission bit joint with external slot, a return spring, a bit body, seals, and alloy teeth. The upper end of the bit joint is used to connect with the DTH hammer through threads. The inner side of
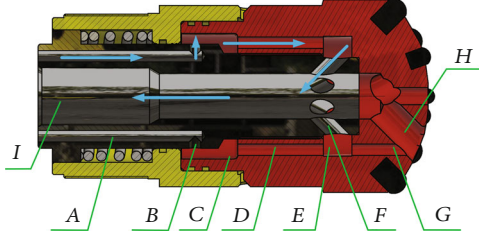
FIGURE 3: Air flow channel and chambers of split reverse circulation bit.

the bit joint is sliding connected with the outside of the upper end of the anvil, and several sliding seals are set between the bit joint and the anvil. The bit body is connected with the bit joint through splines, which can transmit the rotary torque from drill pipes to drill bit. A sliding seal is arranged between the bit body and the bit joint. The bit body is threaded with the lower end of the anvil, and a return spring is arranged under the anvil. When the piston of the DTH air hammer impacts on the anvil, the bit body impacts and breaks the rock at the borehole bottom. Meanwhile, because of the sliding connection between the bit joint and the anvil, the impact on the bit joint can be avoided, so as to ensure the reliability of the threaded connection between the bit joint and the DTH air hammer. Compared to the traditional integral reverse circulation drill bits, the split drill bit decomposes the load it bears into different components. Based on the functions and stress states of the above different components, targeted selection of the materials and strength can reduce the failure rate of vulnerable parts and then improve the service life of drill bits.

In reverse circulation drilling, after compressed air drives the DTH hammer to operate, shown in Figure 3, it flows through the anvil axial inlet holes (a) and radial holes (b) into the bit body chamber (c). Then, the air enters the injection chamber (e) through the exhaust holes (d) of the bit body, where the air flow direction changes and a new potential energy and kinetic energy ratio is obtained after the dynamic quantity exchanging. From the injection chamber (e), the air is sprayed at a high velocity to the hollow exhaust channel (i) through the injection exhaust holes (f). At the same time, a part of high-velocity air reaches the borehole bottom through jet holes (g) to realize cooling the bit teeth and removing cuttings at the borehole bottom. When the air flows through the injection exhaust holes (f), the high-velocity air flow forms a negative pressure in the hollow channel of the anvil, and rock cuttings at borehole bottom are pumped into the central passageway of the anvil through the drill bit slag discharge passageway (h). The central channel (i) of the reverse circulation bit connects to the inner pipe of the DTH hammer and the inner pipes of dual-wall drill pipes. It is used for carrying drill cuttings up by the air to complete reverse circulation drilling.

3. CFD Simulation Analysis of the Split Reverse Circulation Bit

In order to investigate the performance of the reverse circulation split drill bit and analyse its internal passageway struc-
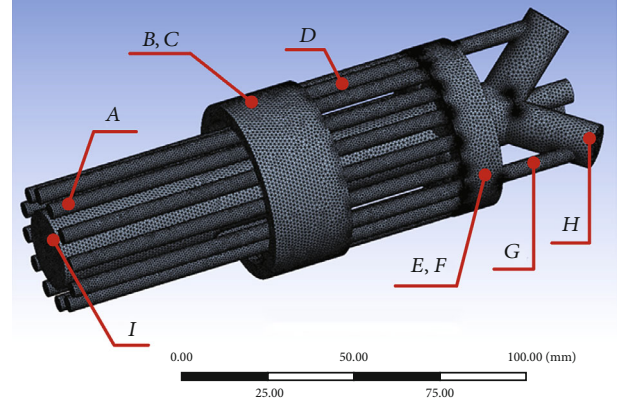

FIGURE 4: Computational domain and mesh division of the split reverse circulation bit.

ture, flow field analysis is carried out based on the software ANSYS.

3.1. Computational Domain and Mesh. According to the structure of the split drill bit, computational domain and mesh division of the split drill bit are obtained, as shown in Figure 4. The maximum outer diameter of the reverse circulation split bit is 135 mm. The computational domain can be divided into anvil axial inflow area (a), anvil radial outflow area (b), annular space gap area between bit body and anvil (c), bit axial inflow area (d), bit body injection chamber (e), anvil injection exhaust holes (f), bit bottom injection holes (g), drill bit cutting discharge holes (h), and central slag discharge channel (i). The size of grid cells is controlled within 2 mm.

3.2. Boundary Conditions. The fluid flow through the split reverse circulation bit follows the laws of physical conservation, including the laws of mass conservation, momentum conservation, and energy conservation [29, 30]. The general governing equations of the above conservation laws are as follows:

$$\frac{\partial(\rho\varnothing)}{\partial t} + \mathrm{div}\,(\rho u\varnothing) = \mathrm{div}\,(\Gamma\,\mathrm{grad}\varnothing) + S. \tag{1}$$

Its expansion form is

$$\begin{aligned}
&\frac{\partial(\rho\varnothing)}{\partial t} + \frac{\partial(\rho u\varnothing)}{\partial x} + \frac{\partial(\rho v\varnothing)}{\partial y} + \frac{\partial(\rho w\varnothing)}{\partial z} \\
&= \frac{\partial}{\partial x}\left(\Gamma\frac{\partial\varnothing}{\partial x}\right) + \frac{\partial}{\partial y}\left(\Gamma\frac{\partial\varnothing}{\partial y}\right) + \frac{\partial}{\partial z}\left(\Gamma\frac{\partial\varnothing}{\partial z}\right) + S,
\end{aligned} \tag{2}$$

where $\varnothing$ can represent u, v, w, and T; u, v, and w are the velocity vectors; Γ is the generalized diffusion coefficient; and S is the generalized source term. Equation (1) is the convection diffusion equation, and the items in it from left to right are transient term, convective term, diffusive term, and source term in turn.

When the DTH air hammer works, the volume flow rate usually changes between $10\,\mathrm{m}^3/\mathrm{min}$ and $30\,\mathrm{m}^3/\mathrm{min}$.

Therefore, the inlet boundary is set as mass flow inlet with the value of 0.204 kg/s, which is equivalent to the volume flow of 10 m^3/min. The outlet pressure of the central channel is atmospheric pressure, and the outlet boundary is set as pressure outlet with the value of 0; that is, the gauge pressure is 0. The wall condition is a static wall without relative slip.

3.3. Solution Methods. The continuity equation, momentum conservation equation, and energy conservation equation are calculated by ANSYS Workbench software. The field characteristics of the compressible gas flowing in the DTH hammer are analyzed based on the Navier-Stokes equation including the turbulence model, with the standard K-ε model and the 3D solver selected. For the separation and coupling algorithms in ANSYS Workbench, there are four available algorithms in the solution methods when using a pressure based solver, which are SIMPLE, SIMPLEC, PISO, and Coupled. The first three are separation algorithm, and the fourth is coupling algorithm. The separation algorithm is a semi-implicit solution to solve the momentum equation and the pressure correction equation, respectively, and thus, its rate of convergence becomes slower. The coupled algorithm solves the continuity equation based on momentum and pressure together, which has more advantages than the separation algorithm in calculating high-speed compressible flow. To consider the interaction of velocity and pressure, the pressure-velocity coupled algorithm is selected as the solution method, with the pseudotransient display factor to ensure the calculation accuracy and rapid convergence. For the spatial discretization schemes, the last squares cell-based discretization scheme was adopted. Turbulent kinetic energy and turbulent dissipation rate are discretized in the first-order upwind space, pressure is discretized in the second-order space, and momentum is discretized in the second-order upwind space. In order to speed up the convergence, pseudotransient display relaxation factors are set as follows: 0.5 for pressure, 0.5 for momentum, 1 for density, 1 for volume force, 0.75 for turbulence kinetic energy, 0.75 for turbulence dissipation rate, and 1 for turbulence viscosity.

4. Simulation Results and Discussion

Take a plane and a line in the central passageway of the split reverse circulation bit and draw its pressure curve, as Figure 5 shows. From the figure, we can find that the pressure at the injection exhaust hole is far less than the pressure at the borehole bottom, and the pressure difference can be more than 20 kPa. This negative pressure can produce enough suction to discharge the drilling cuttings in the borehole, so as to realize reverse circulation drilling. In order to ensure the reverse circulation drilling effectively, the internal gas channel of the bit should be optimized. In this section, the flow field characteristics of the split drill bit are studied, with that the mass flow rate, number of inlet holes, angle of injection exhaust holes, and diameter of injection exhaust holes are considered.

Figure 6 is the velocity nephogram inside the split drill bit. From the figure, we can find that the compressed air flows into the split reverse circulation bit from the axial

holes of the anvil and produces the maximum flow rate when flowing out from the radial holes of the anvil. At the outlet of the injection exhaust holes, relatively high flow rates and low pressure are generated, which is conducive to suction and remove the cuttings at the borehole bottom and realize the reverse circulation drilling. At the same time, vortex is generated near the slag discharge channel, which helps to drive the rock cuttings in the borehole to tumble into the central passageway of the split drill bit.

4.1. Influence of Input Flow Rate on the Flow Characteristics. As one of the most important technical parameters, compressed air flow rate will affect the working performance of air DTH hammer. During the DTH hammer working, its piston is driven by compressed air to reciprocate, which will cause pulsation of gas flow rate in the split drill bit. It is necessary to study the flow field characteristics in the split drill bit when input gas flow rate changes, so as to provide guidance for bit design and engineering application.

In this group of analysis, inlet holes of the anvil with a diameter of 8 mm and quantities of 12 and injection exhaust holes of the split drilling bit with a diameter of 12 mm, quantities of 6, and angle of 45° were chosen. Setting the input gas flow rate to 0.10 kg/s, 0.15 kg/s, 0.20 kg/s, 0.25 kg/s, 0.30 kg/s, 035 kg/s, and 0.40 kg/s, respectively, mass flow rate characteristics out of injection exhaust holes is shown as Figure 7. From the curve, as the mass flow rate flowing into the split drill bit increases, the gas mass flow rate out of the injection exhaust holes increases. However, there are different variation trends for the ratio of the injection exhaust hole outlet mass flow rate to the whole inlet mass flow rate. When the inlet mass flow is 0.25 kg/s, this ratio reaches its maximum value of 83.04%; when the inlet mass flow is 0.3 kg/s, this ratio reaches its minimum value of 82.07%. The maximum value and the minimum value are pretty close, so the ratio can be regarded as unchanged in the range of error permissible. When the bit structure is determined, increasing the inlet air mass flow rate, larger injection flow can be obtained, and the ratio of the injection exhaust hole outlet mass flow rate to the whole inlet mass flow rate is not affected.

When the inlet flow rate is set to 0.10 kg/s, 0.15 kg/s, 0.20 kg/s, 0.25 kg/s, 0.30 kg/s, 035 kg/s, and 0.40 kg/s, respectively, in the simulation, the maximum pressure at the inlet of the split drill bit is illustrated in Figure 8. It can be obtained from the curve that with the gas inlet mass flow rate increasing, maximum pressure at the inlet of the split drill bit gradually increases. Select polynomial fitting, the maximum pressure and inlet flow rate are in a quadratic function relationship, which is

$$y = 4 \times 10^6 x^2 + 67619x - 3148.7, \tag{3}$$

where y is the maximum pressure and x is the inlet flow rate.

In this group of analysis, the maximum pressure increased from 48387.16 Pa to 739856.50 Pa. Due to the fixed size of internal channels of this split bit, increasing the gas inlet flow rate will increase the pressure loss of gas passing through it, therefore influencing the cutting carrying and discharging capacity in the reverse circulation.
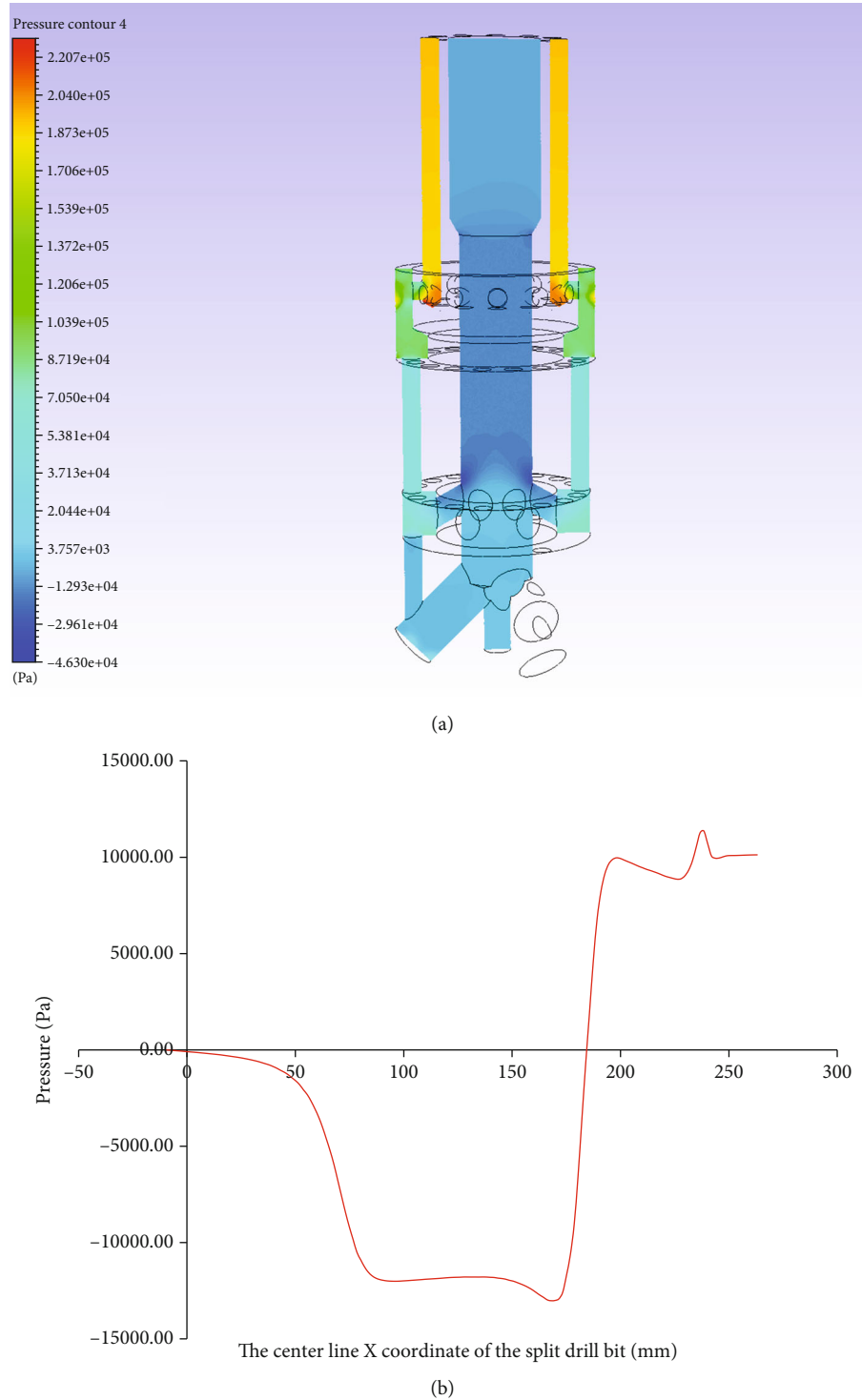
(a)

(b)

FIGURE 5: Pressure of the split reverse circulation bit: (a) pressure nephogram of drill bit profile; (b) pressure at the central line of the drill bit.

4.2. Influence of the Number of Inlet Holes of the Anvil. The air discharged from DTH hammer enters the split bit through axial inlet holes of the anvil. The number of axial inlet holes not only affects the flow field inside the split bit but also affects the strength of the anvil. In this group of flow field analysis, the diameter of the axial inlet holes is 8 mm, and 6 injection exhaust holes with a diameter of 8 mm and an angle of 45° are designed. Figure 9 shows mass flow rate characteristics of

the injection exhaust holes when the number of the axial inlet holes of the anvil is set to 8, 9, 10, 11, 12, 13, and 14, respectively. According to the result curve, it can be obtained that with increasing numbers of axial inlet holes, gas mass flow rate out of injection exhaust holes increases at first, then decreases, and then increases again. Similarly, with the increase of the number of axial inlet holes, the ratio of the injection exhaust hole outlet flow rate to the whole inlet flow rate increases at
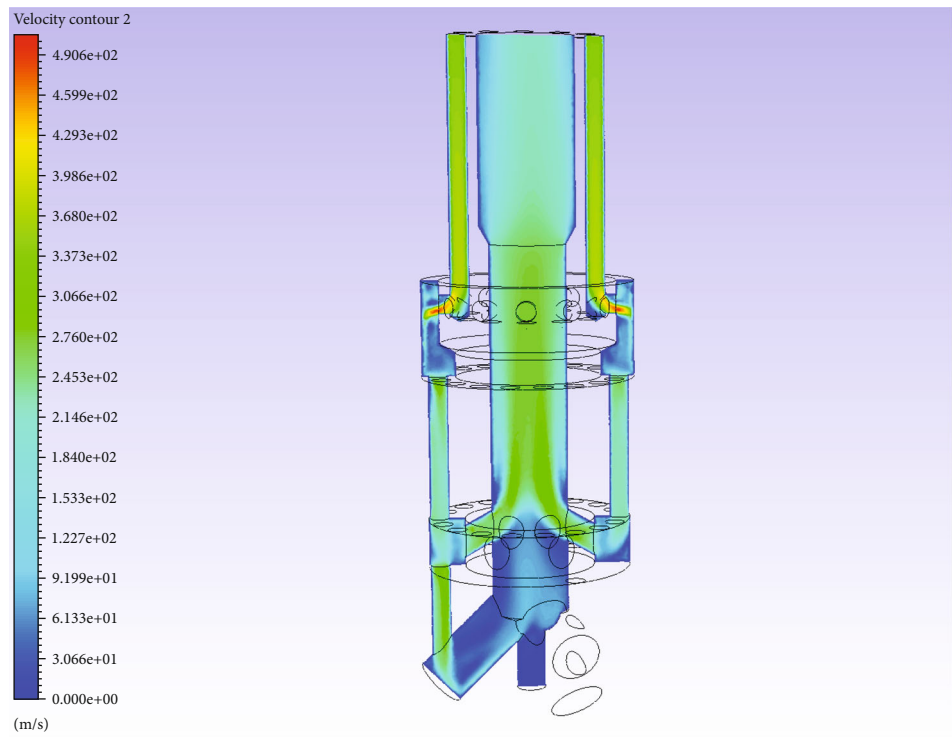
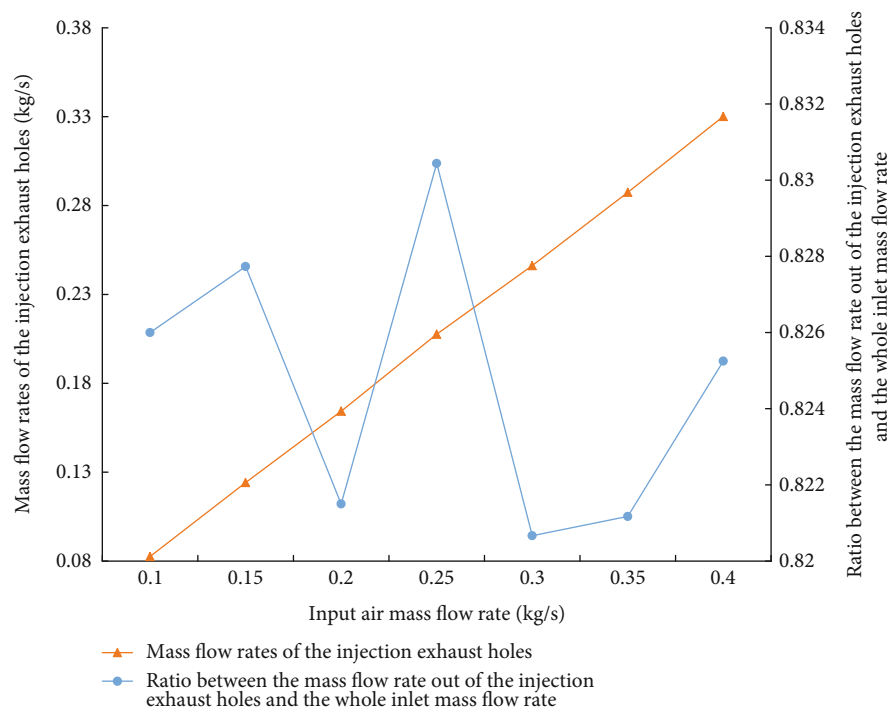FIGURE 6: Velocity nephogram of the drill bit.

FIGURE 7: Flow rate characteristics with different gas inlet mass flow rates.

first, then decreases, and then increases. When there are 8 inlet holes, gas mass flow rate out of injection exhaust holes and the ratio can reach the minimum values of 0.1635 kg/s and 80.14%, respectively; when the number of the inlet holes is 14, the above parameters can reach the maximum value of 0.1675 kg/s and 82.11%.

Figure 10 illustrates the maximum pressure at the split drill bit inlet with different numbers of axial inlet holes.
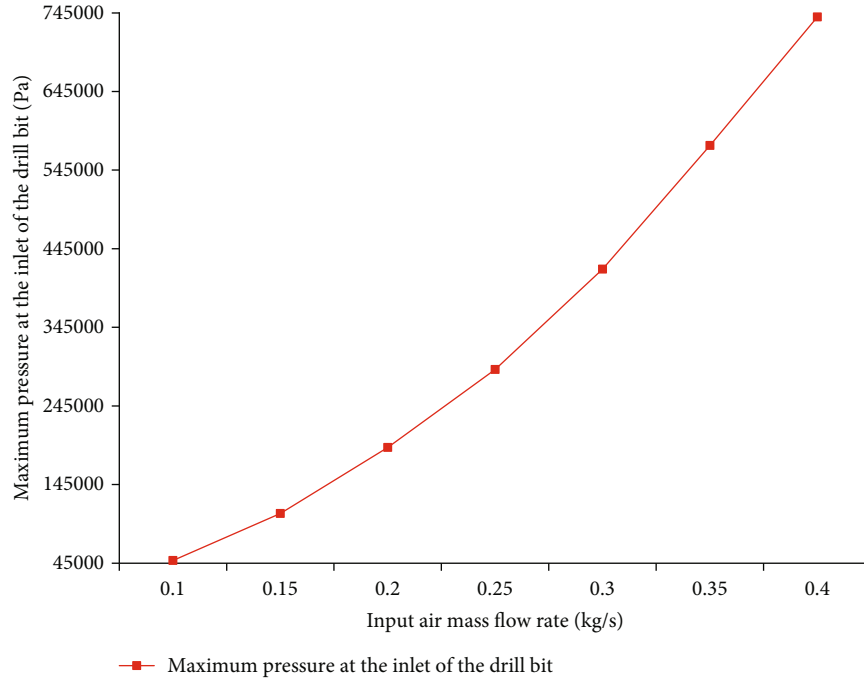
FIGURE 8: Maximum pressure at the inlet of the split bit when inlet flow rate changes.
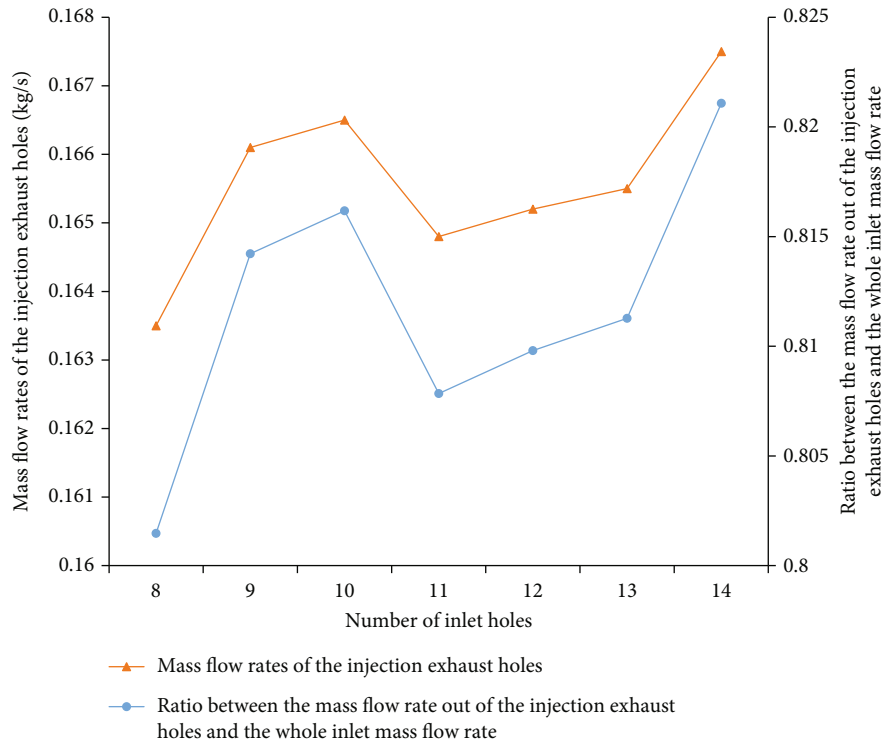

FIGURE 9: Flow rate characteristics with different numbers of axial inlet holes on the anvil.

Based on the figure, we can find that as the number of axial inlet holes increases, the maximum pressure at the split drill bit inlet decreases from 297104.13 Pa to 162309.27 Pa in this group of analysis. The size of the fluid channel flowing into the split drill bit increases due to the number of inlet holes increasing, and when the gas mass flow rate is constant, it

is conducive to air discharge. However, increasing the number of axial inlet holes will reduce the strength of the anvil, so the more numbers of inlet holes are not the better. Considering the injection capacity, pressure loss, and bit strength based on the above results, inlet holes of 10 are recommended to obtain ideal reverse circulation.
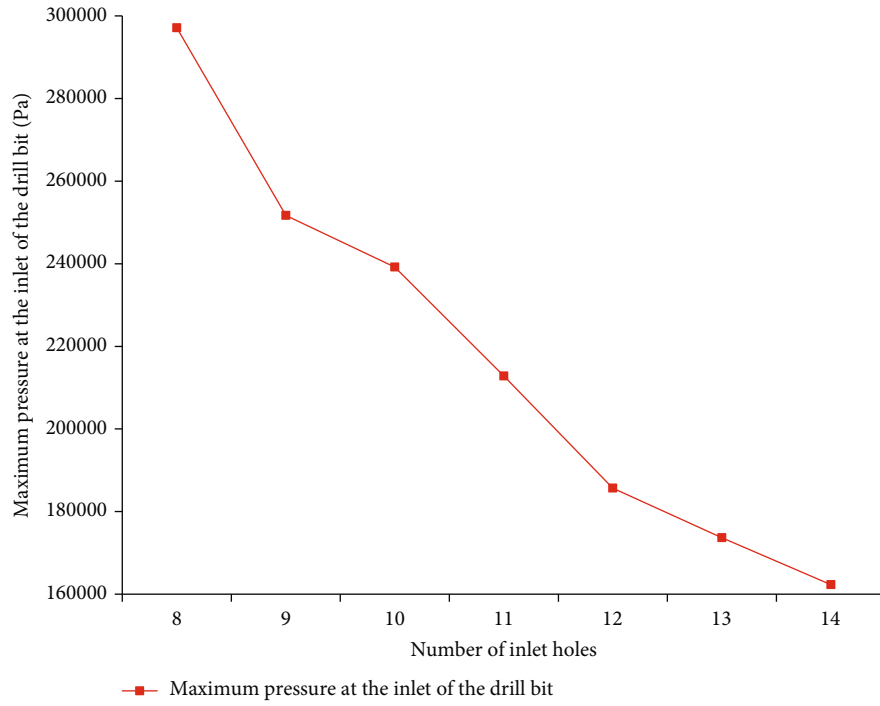
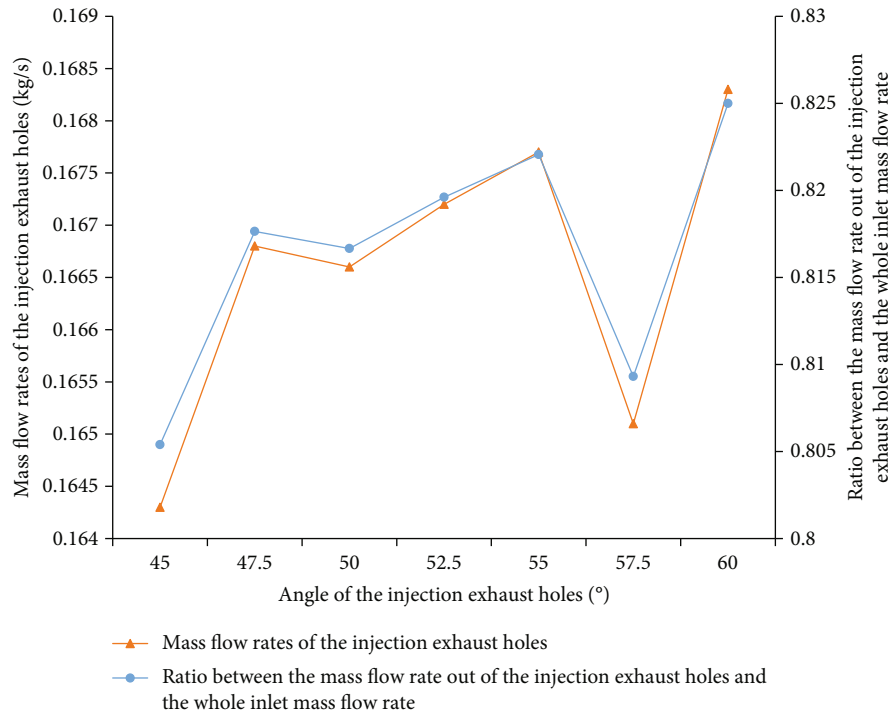FIGURE 10: Maximum pressure at the inlet of the drill bit with different numbers of inlet holes on the anvil.

FIGURE 11: Flow rate characteristics with different angles of injection exhaust holes.

4.3. Influence of Angles of Injection Exhaust Holes. After air enters the split bit through axial holes of the anvil, it will eventually flow into the central passageway inside the split drill bit through its injection exhaust holes and slag discharge holes. The parameters of the injection exhaust holes have significant influence on the flow field characteristics and drilling properties of the split bit. In this group of analysis, the diameter of the axial inlet holes is 8 mm with numbers of 12, and the diameter of the injection exhaust holes is 8 mm with numbers of 6. Setting the angles of the injection
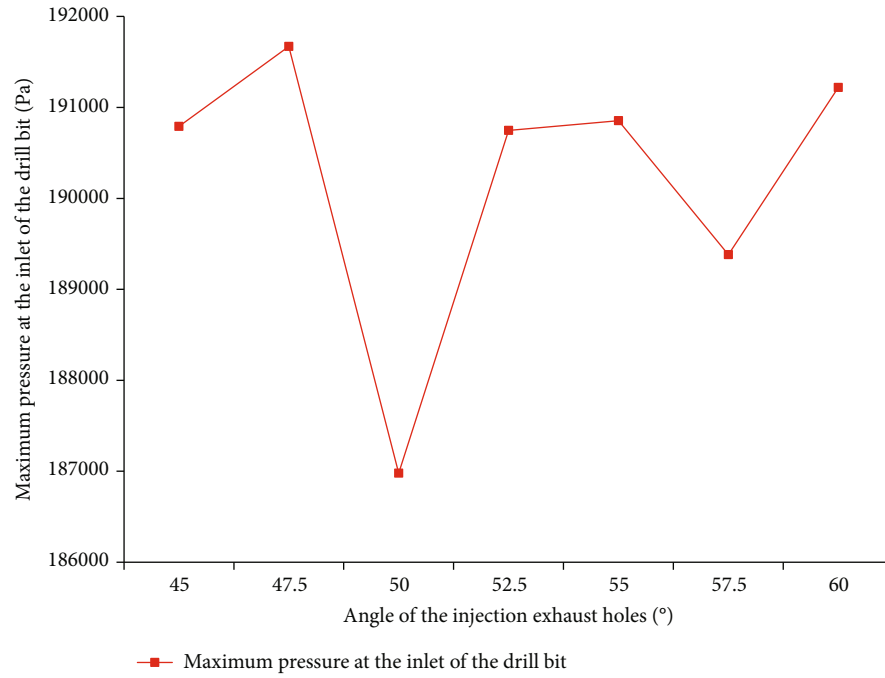
FIGURE 12: Maximum pressure at the inlet of the drill bit with different angles of injection exhaust holes.
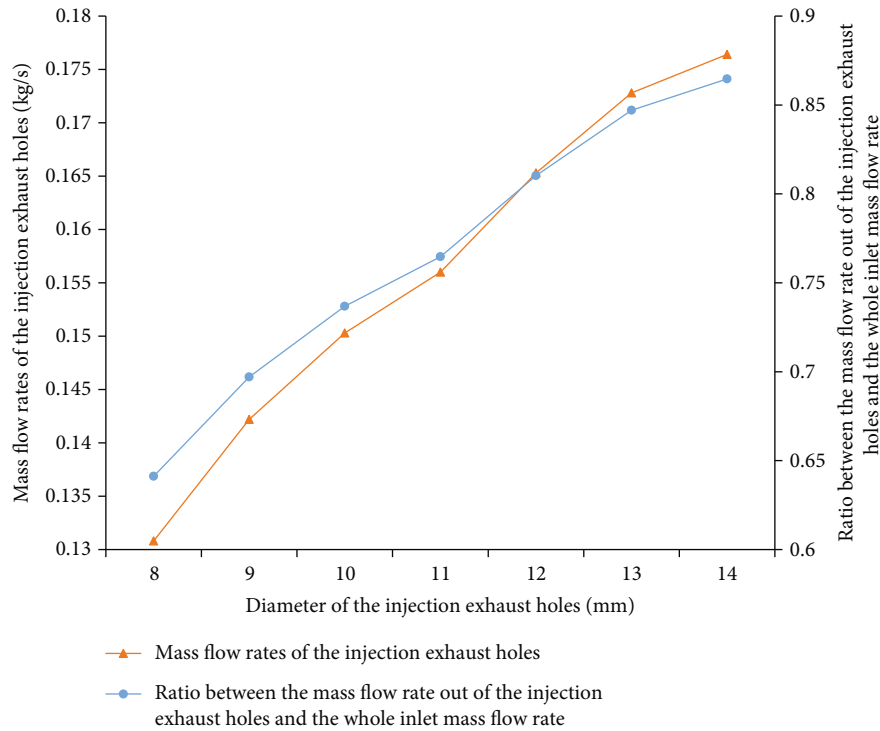

FIGURE 13: Flow rate characteristics with different diameters of injection exhaust holes.

exhaust holes to 45°, 47.5°, 50°, 52.5°, 55°, 57.5°, and 60°, respectively, mass flow rate characteristics of the injection exhaust holes are illustrated in Figure 11. According to the curve, it is obvious that when the injection exhaust hole angles increase, the gas mass flow rate out of the injection exhaust holes increases at first, then decreases, and then increases again. With the increase of angles of the injection exhaust holes, the ratio of the injection exhaust hole outlet mass flow rate to the whole inlet mass flow rate increases in the similar trend. When the angle of the injection exhaust
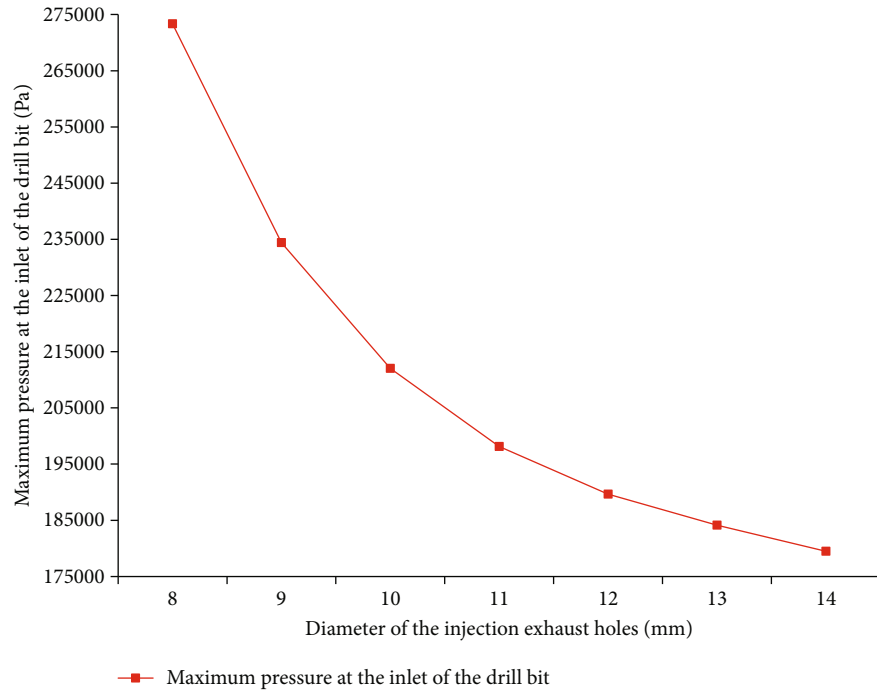
FIGURE 14: Maximum pressure at the split drill bit inlet with different injection exhaust hole diameters.

holes is 45°, the gas mass flow rate and the ratio reach their minimum value of 0.1643 kg/s and 80.54%, respectively; and the above parameters can reach the maximum value of 0.1683 kg/s and 82.50% at the angle of the injection exhaust holes of 60°.

Figure 12 shows the maximum pressure at the split bit inlet when the angles of injection exhaust holes change. It can be obtained from the figure that as the injection exhaust hole angles increase, the maximum pressure at the split drill bit inlet fluctuates. When the angle is 50°, the maximum pressure reaches its minimum value of 186978.62 Pa; and a relatively low value of 189380.36 Pa can be obtained at the angle of 57.5°. Low value of the maximum pressure means low pressure loss, which is conducive to air discharge and cutting removal by reverse circulation. Based on the above analysis results, the recommended injection exhaust hole angle is 50°, for obtaining relatively high injection flow rate and low pressure loss.

4.4. Influence of Diameters of the Injection Exhaust Holes.

In this group of analysis, diameters of the axial inlet holes are 8 mm with numbers of 12, and angles of the injection exhaust holes are 45° with numbers of 6. Setting diameters of the injection exhaust holes as 8 mm, 9 mm, 10 mm, 11 mm, 12 mm, 13 mm, and 14 mm, mass flow rate characteristics of the injection exhaust holes are shown in Figure 13. Based on the figure, we can find that with the increase of diameters of injection exhaust holes, the mass flow rate out of the injection exhaust holes gradually increases from the value of 0.1308 kg/s to 0.1764 kg/s. With the increase of diameters of the injection exhaust holes, the ratio of the injection exhaust hole outlet flow rate to the

FIGURE 15: Different types of split drill bits.

whole inlet mass flow rate changes in the similar trend, increasing from 64.12% to 86.47%.

The maximum pressure at the split drill bit inlet is illustrated in Figure 14 as diameters of the injection exhaust holes change. From the result curve, it can be found that when increasing the diameter of the injection exhaust holes, maximum pressure at the split drill bit inlet will decrease. In this set of analysis, the maximum pressure decreased from 273334.84 Pa to 179486.45 Pa. Reasons for the above results is that, when the diameter of the injection exhaust holes increases, the size of the internal fluid passageway of the split bit increases, and when air flow rate is constant, it is conducive to air discharge. However, increasing the diameter of the injection exhaust holes will reduce the strength of the

(a)   (b)

FIGURE 16: Drilling experiment field: (a) percussion compact bit drilling experiment; (b) reverse circulation bit drilling experiment.

anvil, so it is not always better with more injection exhaust holes. Based on the above analysis results, the recommended injection exhaust hole diameter is 12 mm, as relatively high injection flow and low pressure loss can be obtained.

5. Drilling Experiment

For verifying and optimizing the performance of the split drill bits, several split drill bits designed above were manufacture, shown in Figure 15, and drilling experiments were carried out in Sichuan Province.

The split drill bit drilling experiments were conducted in a deep excavation of Chengdu Haifu Commercial Center, Kehua Middle Road, Chengdu, Sichuan Province, China. From top to bottom, the stratums of the site are as follows: Quaternary Holocene artificial fill layer (Q_4^{dl+ml}), ice water accumulation cohesive soil layer of Quaternary middle lower Pleistocene (Q_{1+2}^{fgl}), and mudstone of Cretaceous Guankou formation (K_{2g}). The Quaternary artificial fill layer is miscellaneous fill with a thickness of 0.8 m to 3.5 m at the upper strata. The lower part of the Quaternary artificial fill layer is plain fill mainly composed of cohesive soil, with loose structure, whose thickness is 1.4 m to 3.8 m. For the ice water accumulation cohesive soil layer of Quaternary middle lower Pleistocene, the upper stratum is clay with a layer thickness of 12.8 m to 14.4 m, in which a small amount of pebbles is contained. The lower part of the Quaternary middle lower Pleistocene is pebble containing cohesive soil with a layer thickness of 0.9 m to 2.8 m, which is mainly composed of granite and sandstone. The pebble particle size is 50 mm to 150 mm, some even more than 200 mm, with medium roundness and pebble content of about 50% to 60%. The mudstone of Cretaceous Guankou formation is extremely soft rock and argillaceous texture structure, which is mainly composed of clay minerals. In drilling engineering, loose formations, particularly gravel formations, pose some of the most challenging drilling conditions. This is because those formations lack consolidation, resulting in weak borehole stability and a higher likelihood of accidents such as bore-

hole collapse, drilling tools sticking, and drilling tools burying. Large particles in those formations have high strength and uneven sizes and distributions, making it difficult to break. Meanwhile, due to the delayed removal of rock cuttings, there will be recurrent fragmentation at the bottom of boreholes, leading to reduced drilling efficiency and elevated wear and tear on drill bit.

The drilling rig used in this drilling experiment was YG-100A anchor borehole rig, which was manufactured by Chengdu Jindi Prospecting Machinery Co., Ltd. The drilling rig adopts full hydraulic power, with a drilling depth of 50 m to 150 m, a drilling diameter of 89 mm to 250 mm, and a motor power of 25 kW, as shown in Figure 16. The DTH hammer used in the drilling experiment can impact bidirectionally, with a diameter of 130 mm, which operated at its rated pressure and rated air volume, with a rated pressure range of 1.0~1.4 MPa and a rated air volume range of 10~20 m³/min. During the experiment, the maximum drilling rate can reach 1.5 m/min, and the drilling time is far less than the auxiliary time in a drilling process. From the drilling experiment, it can be concluded that the split bit has good adaptability for reverse circulation drilling in loose formation.

6. Conclusions

As integral reverse circulation bits are suitable for specific formation and the whole set of DTH hammer needs to be replaced for different drilling conditions, several different split drill bits are designed for normal circulation drilling, reverse circulation drilling, percussion compact drilling, and coring drilling. The conclusions of this study were the following:

(1) The split drill bit designed for reverse circulation DTH hammer is composed of an anvil with stepped cylindrical structure, a torque transmission bit joint with externally slot, a return spring, a bit body, seals, and alloy teeth

(2) When the bit structure is determined, increasing the inlet gas mass flow rate, larger injection flow and pressure loss can be obtained; however, the ratio of the injection exhaust hole outlet mass flow rate to the whole inlet mass flow rate changes between 82.07% and 83.04%, which can be regarded as unchanged in the range of error permissible

(3) When increasing the axial inlet hole numbers, the injection exhaust hole outlet mass flow rate increases at first, then decreases, and then increases again, and the ratio of the injection exhaust hole outlet mass flow rate to the whole inlet mass flow rate changes in the same rules, with a minimum value of 80.14% at 8 inlet holes and a maximum value of 82.11% at 14 inlet holes. The maximum pressure at the split drill bit inlet decreases when increasing the axial inlet hole numbers

(4) As the angle of the injection exhaust holes increases, the injection exhaust hole outlet mass flow rate gradually increases at first, then decreases, and then increases again, and the ratio changes in the similar trend, with a minimum value of 80.54% at the angle of 45° and a maximum value of 82.50% at the angle of 60°. The maximum pressure at the split drill bit inlet fluctuates

(5) For the diameter of the injection exhaust holes, when increasing it, the injection exhaust hole outlet mass flow rate gradually increases, and the ratio of the injection exhaust hole outlet mass flow rate to the whole inlet mass flow rate changes in the similar trend, increasing from 64.12% to 86.47%. The maximum pressure at the split bit inlet gradually decreases

(6) Considering the injection capacity, pressure loss, and bit strength, inlet holes of 10, injection exhaust holes with an angle of 50°, and injection exhaust holes with a diameter of 12 mm are recommended to obtain ideal reverse circulation with relatively high injection flow and low pressure loss

(7) Several types of split drill bits were manufactured, and drilling experiments were carried out in the gravel formation. The maximum drilling rate can reach 1.5 m/min in the drilling experiment. The split drill bit has good adaptability for reverse circulation drilling in loose formation

Data Availability

The data used to support the findings of this study are available from the corresponding author upon request.

Conflicts of Interest

The authors declare that there are no conflicts of interest regarding the publication of this paper.

Acknowledgments

References

[1] Z. Yang, J. Peng, D. Ge, Y. Li, J. Li, and P. Liu, "Mechanical response of stress wave attenuator with layered structure under impact load: experimental and numerical studies," *Journal of Applied Mechanics*, vol. 90, no. 5, article 051003, 2023.

[2] Z. Yang, J. Peng, Y. Li et al., "Study on the response of the steel / poly-ether-ether-ketone layered protective structure for a fluidic DTH hammer," *Journal of Petroleum Science and Engineering*, vol. 208, article 109767, 2022.

[3] D. Brito, R. Gómez, G. Carvajal, L. Reyes-Chamorro, and G. Ramírez, "Identification of impact frequency for down-the-hole drills using motor current signature analysis," *Applied Sciences*, vol. 13, no. 8, p. 4650, 2023.

[4] Y. Li, J. Peng, C. Huang et al., "Multi-fractured stimulation technique of hydraulic fracturing assisted by the DTH-hammer-induced impact fractures," *Geothermics*, vol. 82, pp. 63–72, 2019.

[5] D. Ge, J. Peng, K. Li, C. Huang, M. Lian, and Z. Yang, "Influence of water-based drilling fluids on the performance of the fluidic down-the-hole hammer," *Journal of Petroleum Science and Engineering*, vol. 195, article 107817, 2020.

[6] L. Lou, M. Chen, W. Qin, W. Wu, and H. Rui, "Research on the synchronization and shock characteristics of an air adjustment mechanism for cluster-type DTH hammers under partial loads," *Shock and Vibration*, vol. 2022, Article ID 9794391, 17 pages, 2022.

[7] D. J. Kim, J. Y. Oh, J. W. Cho, J. Kim, J. Chung, and C. Song, "Design study of impact performance of a DTH hammer using PQRSM and numerical simulation," *Journal of Mechanical Science and Technology*, vol. 33, no. 11, pp. 5589–5602, 2019.

[8] J. Peng, D. Ge, X. Zhang, M. Wang, and D. Wu, "Fluidic DTH hammer with backward-impact-damping design for hard rock drilling," *Journal of Petroleum Science and Engineering*, vol. 171, pp. 1077–1083, 2018.

[9] C. Schulz, T. Schläfer, E. Charrault, and C. Hall, "Erosive wear testing of laser clad and HVOF coatings for drilling in mining," *Journal of Thermal Spray Technology*, vol. 29, no. 3, pp. 520–529, 2020.

[10] I. A. Zhukov, B. N. Smolyanitsky, and V. V. Timonin, "Improvement of down-the-hole air hammer efficiency by optimizing shapes of colliding parts," *Journal of Mining Science*, vol. 54, no. 2, pp. 212–217, 2018.

[11] K. Bo, S. Sun, Y. Hu, and M. Wang, "Design optimization and performance analysis of the pneumatic DTH hammer with self-propelled round bit," *Shock and Vibration*, vol. 2021, Article ID 6653390, 13 pages, 2021.

[12] X. Zhang, Y. Luo, X. Gan, and K. Yin, "Design and numerical analysis of a large-diameter air reverse circulation drill bit for

reverse circulation down-the-hole air hammer drilling," *Energy Science & Engineering*, vol. 7, no. 3, pp. 921–929, 2019.

[13] L. Liu, J. Zhou, L. Kong, Y. Wang, and J. Li, "Analysis of the dynamic response and impact parameters of pneumatic down-the- hole hammer drilling rescue holes," *Geoenergy Science and Engineering*, vol. 228, article 211935, 2023.

[14] J. He, Z. Q. Zhao, Q. L. Yin, Y. J. Luo, and X. Gan, "Design and optimisation on rapid rescue well-drilling technology with large-diameter pneumatic hammers," *International Journal of Mining, Reclamation and Environment*, vol. 34, no. 1, pp. 19–33, 2020.

[15] X. Zhang, Z. Wu, Z. Zhao, P. Sun, L. Tang, and U. Shabir, "Insight into dust control performance of a reverse circulation drill bit using multiphase flow simulation," *Engineering Applications of Computational Fluid Mechanics*, vol. 16, no. 1, pp. 841–857, 2022.

[16] B. Qi, P. Cao, H. Yang et al., "Experimental and numerical study on air flow behavior for a novel retractable reverse circulation drill bit of casing-while-drilling (CwD)," *Geofluids*, vol. 2021, Article ID 3586572, 12 pages, 2021.

[17] R. Ershadnia, M. A. Amooie, R. Shams et al., "Non-Newtonian fluid flow dynamics in rotating annular media: physics-based and data-driven modeling," *Journal of Petroleum Science and Engineering*, vol. 185, article 106641, 2020.

[18] P. Cai, W. Nie, D. Chen, S. Yang, and Z. Liu, "Effect of air flow-rate on pollutant dispersion pattern of coal dust particles at fully mechanized mining face based on numerical simulation," *Fuel*, vol. 239, pp. 623–635, 2019.

[19] M. N. A. Zico, M. A. Rahman, H. B. Yusuf, and M. M. Rahman, "CFD modeling of drill cuttings transport efficiency in annular bends: effect of hole eccentricity and rotation," *Geoenergy Science and Engineering*, vol. 221, article 211380, 2023.

[20] C. Feng, W. Liu, and D. Gao, "CFD simulation and optimization of slurry erosion of PDC bits," *Powder Technology*, vol. 408, article 117658, 2022.

[21] S. Sun, K. Bo, R. Jia, P. Cao, B. Chen, and M. Guo, "Experimental investigation and CFD simulation of multiphase flow behavior in air reverse circulation drilling," *Advanced Powder Technology*, vol. 34, no. 10, article 104168, 2023.

[22] K. Wu and Z. Ye, "The numerical research on rock breaking and rising mechanism of rotary-percussive drilling," *Arabian Journal for Science and Engineering*, vol. 44, no. 12, pp. 10561–10580, 2019.

[23] D. Bai, Q. Quan, Y. Wang, H. Li, P. Zhao, and Z. Deng, "Impact dynamics prediction of a rotary-percussive ultrasonic drill with a free mass," *IEEE Access*, vol. 6, pp. 32649–32661, 2018.

[24] W. Liu, X. Zhu, and B. Li, "The rock breaking mechanism analysis of rotary percussive cutting by single PDC cutter," *Arabian Journal of Geosciences*, vol. 11, no. 9, p. 192, 2018.

[25] Y. Wang, Q. Quan, H. Yu, D. Bai, H. Li, and Z. Deng, "Rotary-percussive ultrasonic drill: an effective subsurface penetrating tool for minor planet exploration," *IEEE Access*, vol. 6, pp. 37796–37806, 2018.

[26] Z. Chen and M. Bian, "Dynamic centrifuge test and numerical modelling of the seismic response of the tunnel in cohesive soil foundation," *Buildings*, vol. 12, no. 3, p. 337, 2022.

[27] X. Zhang, Y. Luo, L. Fan, J. Peng, and K. Yin, "Investigation of RC-DTH air hammer performance using CFD approach with dynamic mesh method," *Journal of Advanced Research*, vol. 18, pp. 127–135, 2019.

[28] C. Mao, X. Zhang, F. Li, D. Wu, and S. Zhang, "On cutting transport for air reverse circulation in horizontal and inclined wells," *Tunnelling and Underground Space Technology*, vol. 136, article 105095, 2023.

[29] P. Cao, Y. Chen, M. Liu, and B. Chen, "Optimal design of novel drill bit to control dust in down-the-hole hammer reverse circulation drilling," *Arabian Journal for Science and Engineering*, vol. 43, no. 3, pp. 1313–1324, 2018.

[30] D. Kim, J. Kim, B. Lee et al., "Prediction model of drilling performance for percussive rock drilling tool," *Advances in Civil Engineering*, vol. 2020, Article ID 8865684, 13 pages, 2020.